Research Paper
Computational Methods for Differential Equations
http://cmde.tabrizu.ac.ir
Vol. *, No. *, *, pp. 1-13
DOI:10.22034/cmde.2026.68172.3290

Optimal solution of kidney function model via fractional clique polynomials neural network

H. Hassani[1,*], Z. Avazzadeh[2], Sh. Ezzatzadegan Jahromi[3], and M. J. Ebadi[4]

[1]Department of Mathematics, Anand International College of Engineering, Jaipur 303012, India.

[2]Stony Brook Institute at Anhui University, Anhui University, Hefei 230601, China.

[3]Department of Medicine, School of Medicine, Shiraz Nephro-Urology Research Center, Shiraz University of Medical Sciences, Shiraz, Iran.

[4]DICEAM Department, Mediterranean University of Reggio Calabria, Via Graziella Feo di Vito, 89060 Reggio Calabria, Italy.

Abstract

We propose the fractional clique polynomials neural network (FCPNN), a hybrid architecture integrating neural networks with fractional clique polynomials (FCPs), to solve mathematical kidney function models (MKFMs) critical for clinical disease modeling. The FCPNN method employs time (in months) as an input variable, with FCPs as activation functions in the hidden layer and the arcsinh(t) function in the output layer, enhancing adaptability to nonlinear biological dynamics. We rigorously establish the method's theoretical foundations through convergence analysis and proofs of solution existence and uniqueness. By incorporating Lagrange multipliers for optimization, FCPNN improves constraint handling and prediction accuracy. This work advances computational tools for kidney disease modeling, offering a robust framework for personalized medical applications.

Keywords. Fractional clique polynomials neural network, Mathematical kidney function model, Optimization algorithm.

2010 Mathematics Subject Classification. 34A08, 68T07, 65L05.

1. Introduction

Water is fundamental to life and critical for hydration, food preparation, sanitation, and hygiene. The primary objective of drinking water supply systems is to safeguard human health by ensuring access to adequate supplies of safe water [17]. Total water hardness is defined as the sum of temporary (carbonate) hardness and permanent (non-carbonate) hardness[6]. Research underscores the significant role of magnesium in hypertension, cardiac electrical disorders, arrhythmias, and cardiovascular health [6]. Similarly, dietary calcium intake has been linked to a reduced risk of cardiovascular events associated with high blood pressure, as calcium supports stronger heart muscle contractions. Given that hard water can provide up to 9% of daily calcium intake, mineral-rich water may serve as a valuable dietary supplement for calcium and magnesium [6]. Epidemiological studies have shown a distinct association between drinking water composition and cardiovascular diseases, with incidence rates 10–30% higher in regions with soft water compared to areas with hard water [21]. A study in Iran further revealed a significantly higher prevalence of hypertension (HTN) and prehypertension in areas with low water hardness relative to high-hardness regions [21]. Additionally, research suggests that prolonged exposure to soft water may elevate the risk of Alzheimer's disease and vascular dementia [2].

Kidney stone disease remains a major global public health challenge. Water hardness, determined primarily by calcium and magnesium content, has been studied as a potential environmental risk factor influencing kidney stone formation. However, prior investigations into this relationship have produced conflicting results, with some studies reporting a positive correlation and others finding no significant association [20]. A recent prospective cohort study in the UK, analyzing data from 288,041 UK Biobank participants (2006–2024) without prior kidney stone history,

Received: 15 July 2025; Accepted:30 April 2026.
∗ Corresponding author. Email: hosseinhassani40@yahoo.com.

found that higher magnesium levels in drinking water were associated with a reduced risk of kidney stone formation. Nonetheless, no significant link was observed between domestic water hardness, calcium concentration, calcium carbonate levels, and kidney stone incidence in the overall population [20].

Ordinary differential equations (ODEs) have become increasingly vital for modeling biological systems due to their ability to capture complex dynamics. However, obtaining analytical solutions for such models remains challenging, prompting the development of diverse numerical methods. Prakash et al. introduced an extended Haar wavelets-based numerical method to solve a nonlinear fractional dengue model[15]. Ullah et al. devised a numerical technique using the product-integration rule for a fractional tuberculosis model with nonsingular derivative operators[18]. Jasevicius conducted a numerical analysis via the discrete element method to study the mechanics of red blood cell interactions with vessel walls[7]. He et al. applied a neural network algorithm to lung cancer imaging, offering insights for advancing artificial neural networks in medical diagnostics[5]. Movahedi formulated a Susceptible-High risk-Infective-Recovered-Vaccinated (SHIRV) model and provided approximate solutions using the Legendre-Ritz-Galerkin method[13].

Li et al. developed a mechanical model for red blood cells, incorporating the complex structure of blood vessels through an unstructured grid approach to study flow dynamics in intricate vascular systems[11]. Jeeva and Dharmalingam employed three analytical methods—the transcendental-exponential method, Homotopy perturbation method, and higher-order inverse polynomial method—to derive approximate solutions for a nonlinear tuberculosis model within an SEITR framework[8]. Asadi-Mehregan et al. performed numerical simulations of spatio-temporal infectious disease spread using a collocation method based on local radial basis functions[1]. Chen et al. analyzed an age-structured SIS model through the linearly implicit Euler method[3].

Pandey and Ghosh proposed a three-dimensional childhood disease model with Caputo operators, establishing existence and uniqueness conditions for solutions[14]. Li and Yang implemented the linearly implicit Euler method for an age-structured HIV model incorporating latently infected T cells[9]. Wang et al. extended this approach to numerically represent an age-structured HIV infection model with a generalized transmission mechanism[19]. He pioneered the use of extreme learning machines, a neural network technique, to solve dynamic models of CD4(+) cells in HIV infection[4]. Consider the following mathematical kidney function model:

$$\begin{cases} \frac{dS(t)}{dt} = a - \beta\left(\frac{W(t)}{W(t)+k}\right)S(t) - \mu S(t), \\ \frac{dI(t)}{dt} = \beta\left(\frac{W(t)}{W(t)+k}\right)S(t) - (\gamma+\mu)I(t), \\ \frac{dR(t)}{dt} = \gamma I(t) - \mu R(t), \\ \frac{dW(t)}{dt} = bW(t)\left(1 - \frac{W(t)}{k}\right) - cW(t), \\ S(0) = S_0 \geq 0, \quad I(0) = I_0 \geq 0, \quad R(0) = R_0 \geq 0, \quad W(0) = W_0 \geq 0, \end{cases} \tag{1.1}$$

where susceptible, infected and recovered human populations are denoted as $S(t)$, $I(t)$ and $R(t)$ respectively, and water components are represented as $W(t)$. A description of parameters for the model (1.1) is provided in Table 1.

TABLE 1. Definition of parameters in model (1.1).

Parameter	Description
a	the human population using the susceptible birth
β	the magnesium and calcium ratio of water
k	the limited enhanced compound (calcium, magnesium) water
μ	the coefficient of dental infection transmission
γ	the recovered part
b	the concentration of compound (calcium, magnesium) water
c	the treating water procedure reasons a decrement using the compounds (magnesium, calcium)

Neural networks are neurologically inspired computational systems designed to model complex systems through interconnected neurons, frequently employed for processing intricate datasets. A neural network typically comprises an input layer, one or more hidden layers, and an output layer. The input layer, being the first layer, receives input values and transmits them to the hidden layers. Neurons in the hidden layer process the input data through various

mathematical operations. Each neuron in the hidden layer is fully connected to all neurons in the adjacent layers. In this work, we extend this framework by designing a neural network architecture based on fractional clique polynomials (FCPs) to solve the mathematical kidney function model. The unknown functions $S(t)$, $I(t)$, $R(t)$ and $W(t)$ are expressed as a series expansion using FCPs. The independent variable t serves as the input layer of the network. Within the hidden layer, a perceptron is formulated by employing varying degrees of FCPs and unit weights. The arcsinh(t) activation functions are implemented in the output layer. The rationale behind developing the FCPNN lies in interpreting its output as the differential equation's solution, achieved through approximation with FCPs of varying degrees.

This study focuses on achieving the following objectives:
(i) Propose a neural network method for solving the mathematical kidney function model using fractional clique polynomials (FCPs).
(ii) Introduce the novel concept of FCPs, a generalized extension of Clique polynomials, for the first time.
(iii) Establish the convergence analysis, existence, and uniqueness of solutions for the proposed method.
(iv) Derive an optimization algorithm using the Lagrange multiplier method.
(v) Achieve high accuracy by utilizing truncated series of FCPs.
(vi) Transform the problem under consideration into a system of algebraic equations solvable via numerical techniques.
(vii) Develop a computationally efficient approach applicable in any programming language.
(viii) Validate the method's accuracy through numerical examples.
The remainder of this paper is organized as follows:
Section 2 describes clique polynomials, FCPs, and the fractional clique polynomial neural network (FCPNN).
Section 3 details the FCPNN architecture and the proposed method for solving the kidney function model.
Section 4 provides the convergence analysis and proves the existence and uniqueness of solutions for system (1.1).
Section 5 validates theoretical results through numerical simulations and practical case studies.
Section 6 concludes the work and discusses future directions.

2. Clique polynomials, fractional clique polynomials and function approximation

In this part of the paper, we discuss the definitions of CPs, FCPs and the concept of function approximation using FCPs.

Definition 2.1. The CPs of a graph $\mathscr{G}$ denoted by $\mathscr{C}(\mathscr{G},\tau)$ are defined as [16]:

$$\mathscr{C}(\mathscr{G},\tau)=\sum_{k=0}^{n}c_k(\mathscr{G})\tau^k, \qquad c_0(\mathscr{G})=1, \tag{2.1}$$

where $c_r(\mathscr{G})$ is the number of k-cliques of $\mathscr{G}$. The CPs of a complete graph $\mathscr{H}_n$ with n vertices are defined by [16]:

$$\mathscr{C}(\mathscr{H}_n,\tau)=(1+\tau)^n=\sum_{k=0}^{n}\binom{n}{k}\tau^k. \tag{2.2}$$

Definition 2.2. The FCPs $\mathbf{C}(\mathscr{H}_n,\tau)$ are defined by the change of variable τ^k into $\tau^{k+\alpha_k}$ (where $k+\alpha_k>0$) on CPs as:

$$\mathbf{C}(\mathscr{H}_n,\tau)=\sum_{k=0}^{n}\binom{n}{k}\tau^{k+\alpha_k}, \qquad n\in\mathbb{N}_0,\ \alpha_0=0, \tag{2.3}$$

where α_k denotes control parameter. When $\alpha_k=0$, the FCPs coincide with the classical CPs.

The first FCPs are given by:

$$\begin{cases}\mathbf{C}(\mathscr{H}_0,\tau)=1,\\ \mathbf{C}(\mathscr{H}_1,\tau)=1+\tau^{1+\alpha_1},\\ \mathbf{C}(\mathscr{H}_2,\tau)=1+2\tau^{1+\alpha_1}+\tau^{2+\alpha_2},\\ \mathbf{C}(\mathscr{H}_3,\tau)=1+3\tau^{1+\alpha_1}+3\tau^{2+\alpha_2}+\tau^{3+\alpha_3}.\end{cases} \tag{2.4}$$

The functions $S(t)$, $I(t)$, $R(t)$ and $W(t)$ in Eq. (1.1) can be expressed in the following matrix form:

$$\begin{cases} S(t) \simeq \mathbf{A}^T \mathbf{L}_{m_1}(t) = \mathbf{A}^T \mathfrak{U} \mathbf{H}_{m_1}(t), \\ I(t) \simeq \mathbf{B}^T \mathbf{L}_{m_2}(t) = \mathbf{B}^T \mathfrak{V} \mathbf{H}_{m_2}(t), \\ R(t) \simeq \mathbf{D}^T \mathbf{L}_{m_3}(t) = \mathbf{D}^T \mathfrak{P} \mathbf{H}_{m_3}(t), \\ W(t) \simeq \mathbf{E}^T \mathbf{L}_{m_4}(t) = \mathbf{E}^T \mathfrak{Q} \mathbf{H}_{m_4}(t), \end{cases} \tag{2.5}$$

where

$$\mathbf{A}^T = [a_0\ a_1 \dots a_{m_1}], \quad \mathbf{B}^T = [b_0\ b_1 \dots b_{m_2}], \quad \mathbf{D}^T = [d_0\ d_1 \dots d_{m_3}], \quad \mathbf{E}^T = [e_0\ e_1 \dots e_{m_4}], \tag{2.6}$$

$$\mathfrak{U} = \begin{pmatrix} 1 & 0 & 0 & \cdots & 0 \\ u_{1,0} & u_{1,1} & u_{1,2} & \cdots & u_{1,m_1} \\ \vdots & \vdots & \vdots & \cdots & \vdots \\ u_{m_1,0} & u_{m_1,1} & u_{m_1,2} & \cdots & u_{m_1,m_1} \end{pmatrix}, \quad \mathfrak{V} = \begin{pmatrix} 1 & 0 & 0 & \cdots & 0 \\ v_{1,0} & v_{1,1} & v_{1,2} & \cdots & v_{1,m_2} \\ \vdots & \vdots & \vdots & \cdots & \vdots \\ v_{m_2,0} & v_{m_2,1} & v_{m_2,2} & \cdots & v_{m_2,m_2} \end{pmatrix}, \tag{2.7}$$

$$\mathfrak{P} = \begin{pmatrix} 1 & 0 & 0 & \cdots & 0 \\ p_{1,0} & p_{1,1} & p_{1,2} & \cdots & p_{1,m_3} \\ \vdots & \vdots & \vdots & \cdots & \vdots \\ p_{m_3,0} & p_{m_3,1} & p_{m_3,2} & \cdots & p_{m_3,m_3} \end{pmatrix}, \quad \mathfrak{Q} = \begin{pmatrix} 1 & 0 & 0 & \cdots & 0 \\ q_{1,0} & q_{1,1} & q_{1,2} & \cdots & q_{1,m_4} \\ \vdots & \vdots & \vdots & \cdots & \vdots \\ q_{m_4,0} & q_{m_2,1} & q_{m_4,2} & \cdots & q_{m_4,m_4} \end{pmatrix}, \tag{2.8}$$

$$u_{ij} = \begin{cases} \binom{i}{j}, & i > j, \\ 0, & i \le j. \end{cases} \quad i = 1, 2, \dots, m_1, \quad j = 0, 1, \dots, m_1, \tag{2.9}$$

$$v_{ij} = \begin{cases} \binom{i}{j}, & i > j, \\ 0, & i \le j. \end{cases} \quad i = 1, 2, \dots, m_2, \quad j = 0, 1, \dots, m_2, \tag{2.10}$$

$$p_{ij} = \begin{cases} \binom{i}{j}, & i > j, \\ 0, & i \le j. \end{cases} \quad i = 1, 2, \dots, m_3, \quad j = 0, 1, \dots, m_3, \tag{2.11}$$

$$q_{ij} = \begin{cases} \binom{i}{j}, & i > j, \\ 0, & i \le j. \end{cases} \quad i = 1, 2, \dots, m_4, \quad j = 0, 1, \dots, m_4, \tag{2.12}$$

and

$$\mathbf{H}_{m_i}(t) \triangleq [h_0^i(t)\ \ h_1^i(t) \dots h_{m_i}^i(t)]^T, \qquad i = 1, 2, 3, 4, \tag{2.13}$$

where

$$h_j^i(t) = \begin{cases} 1, & j = 0, \\ t^{j+\alpha_j^i}, & j = 1, 2, \dots, m_i, \end{cases} \qquad i = 1, 2, 3, 4, \tag{2.14}$$

with α_j^i representing the control parameters.

2.1. **Fractional clique polynomials neural network.** In order to efficiently and accurately solve a mathematical kidney function model, a novel FCPNN method is proposed in this paper. The FCPNN method is structured with three layers that function as described below:
(i) The input t is provided by the network's input layer.
(ii) In the network's hidden layer, we select FCPs of varying degrees as activation functions.
(iii) The network's output layer combines FCPs with varying weights in a linear manner, and an activation function is then applied to this combination to generate the output. In this context, arcsine hyperbolic functions are used as activation functions. Consequently, the following are the results of the FCPNN, using input data t and parameters $\mathbf{A}$, $\mathbf{B}$, $\mathbf{D}$, and $\mathbf{E}$:

$$\mathbf{S}(t,\mathbf{A}) = arcsinh(S(t)), \mathbf{I}(t,\mathbf{B}) = arcsinh(I(t)), \quad \mathbf{R}(t,\mathbf{D}) = arcsinh(R(t)), \quad \mathbf{W}(t,\mathbf{E}) = arcsinh(W(t)), \tag{2.15}$$

where $S(t)$, $I(t)$, $R(t)$ and $W(t)$ are a linear combination expressed as:

$$S(t) = \sum_{i=0}^{m_1} b_i \mathbf{L}_i(t), \qquad I(t) = \sum_{j=0}^{m_2} c_j \mathbf{L}_j(t), \qquad R(t) = \sum_{k=0}^{m_3} d_k \mathbf{L}_k(t), \qquad W(t) = \sum_{k=0}^{m_4} e_k \mathbf{L}_k(t), \tag{2.16}$$

and also $\mathbf{B}$, $\mathbf{C}$, $\mathbf{D}$ and $\mathbf{L}$ vectors given by:

$$\mathbf{A}^T = [a_0\ a_1 \dots a_{m_1}], \quad \mathbf{B}^T = [b_0\ b_1 \dots b_{m_2}], \quad \mathbf{D}^T = [d_0\ d_1 \dots d_{m_3}], \quad \mathbf{E}^T = [e_0\ e_1 \dots e_{m_4}]. \tag{2.17}$$

3. Description of the approach

This section focuses on introducing the FCPNN approach for solving the mathematical kidney function model presented in Eq. (1.1). We approximate $S(t)$, $I(t)$, $R(t)$ and $W(t)$ using the following activation functions:

$$\begin{cases} S(t) \simeq \tilde{S}(t) = S_0 + t\mathbf{S}(t,\mathbf{A}), \\ I(t) \simeq \tilde{I}(t) = I_0 + t\mathbf{I}(t,\mathbf{B}), \\ R(t) \simeq \tilde{R}(t) = R_0 + t\mathbf{R}(t,\mathbf{D}), \\ W(t) \simeq \tilde{W}(t) = W_0 + t\mathbf{W}(t,\mathbf{E}). \end{cases} \tag{3.1}$$

We recognize that $S(t)$, $I(t)$, $R(t)$ and $W(t)$ satisfy the initial conditions. By applying Eqs. (3.1) to the initial conditions of problem (1.1), we obtain the following results:

$$\Delta_1 \triangleq \tilde{S}(0) - S_0 \simeq 0, \quad \Delta_2 \triangleq \tilde{I}(0) - I_0 \simeq 0, \quad \Delta_3 \triangleq \tilde{R}(0) - R_0 \simeq 0, \quad \Delta_4 \triangleq \tilde{W}(0) - W_0 \simeq 0. \tag{3.2}$$

By substituting the approximations from (3.1) into (1.1), we obtain:

$$\begin{cases} \frac{d\tilde{S}(t)}{dt} - a + \beta\left(\frac{\tilde{W}(t)}{\tilde{W}(t)+k}\right)\tilde{S}(t) + \mu\tilde{S}(t) \triangleq \mathscr{R}_1(t,\mathbf{A},\mathbf{Q}^1), \\ \frac{d\tilde{I}(t)}{dt} - \beta\left(\frac{\tilde{W}(t)}{\tilde{W}(t)+k}\right)\tilde{S}(t) + (\gamma+\mu)\tilde{I}(t) \triangleq \mathscr{R}_2(t,\mathbf{B},\mathbf{Q}^2), \\ \frac{d\tilde{R}(t)}{dt} - \gamma\tilde{I}(t) + \mu\tilde{R}(t) \triangleq \mathscr{R}_3(t,\mathbf{D},\mathbf{Q}^3), \\ \frac{d\tilde{W}(t)}{dt} - b\tilde{W}(t)\left(1 - \frac{\tilde{W}(t)}{k}\right) + c\tilde{W}(t) \triangleq \mathscr{R}_4(t,\mathbf{E},\mathbf{Q}^4). \end{cases} \tag{3.3}$$

Here $\mathbf{A}$, $\mathbf{B}$, $\mathbf{D}$ and $\mathbf{E}$ represent unknown free coefficients. Furthermore, $\mathbf{Q}^i$ $(i = 1,2,3,4)$ are unknown control parameters defined as follows:

$$\mathbf{Q}^i = \left[\alpha_1^i\ \ \alpha_2^i\ \dots\ \alpha_{m_i}^i\right], \quad i = 1,2,3,4. \tag{3.4}$$

The 2-norm of the residual functions is given by:

$$\mathfrak{R}(\mathbf{A},\mathbf{B},\mathbf{D},\mathbf{E},\mathbf{Q}^1,\mathbf{Q}^2,\mathbf{Q}^3,\mathbf{Q}^4) = \int_0^T \left(\mathscr{R}_1^2(t,\mathbf{A},\mathbf{Q}^1) + \mathscr{R}_2^2(t,\mathbf{B},\mathbf{Q}^2) + \mathscr{R}_3^2(t,\mathbf{D},\mathbf{Q}^3) + \mathscr{R}_4^2(t,\mathbf{E},\mathbf{Q}^4)\right) dt. \tag{3.5}$$

The unknown vectors $\mathbf{A}$, $\mathbf{B}$, $\mathbf{D}$, $\mathbf{E}$, $\mathbf{Q}^1$, $\mathbf{Q}^2$, $\mathbf{Q}^3$, and $\mathbf{Q}^4$ need to be evaluated using the following optimization problem:

$$\min\ \mathfrak{R}\left(\mathbf{A},\mathbf{B},\mathbf{D},\mathbf{E},\mathbf{Q}^1,\mathbf{Q}^2,\mathbf{Q}^3,\mathbf{Q}^4\right), \tag{3.6}$$

under the conditions outlined in Eqs. (3.2), where $\mathfrak{R}$ represents the objective function. To solve this optimization problem, we make the following assumptions:

$$\mathcal{J}^*[\mathbf{A},\mathbf{B},\mathbf{D},\mathbf{E},\mathbf{Q}^1,\mathbf{Q}^2,\mathbf{Q}^3,\mathbf{Q}^4,\theta] = \mathfrak{R}\big(\mathbf{A},\mathbf{B},\mathbf{D},\mathbf{E},\mathbf{Q}^1,\mathbf{Q}^2,\mathbf{Q}^3,\mathbf{Q}^4\big) + \theta\,\Delta. \tag{3.7}$$

It is important to note that θ is the vector of Lagrange multipliers. By applying the Lagrange multiplier technique, we can obtain the necessary and sufficient conditions for optimality, which are as follows:

$$\begin{cases} \dfrac{\partial \mathcal{J}^*}{\partial \theta} = 0, & \dfrac{\partial \mathcal{J}^*}{\partial \mathbf{A}} = 0, & \dfrac{\partial \mathcal{J}^*}{\partial \mathbf{B}} = 0, \\ \dfrac{\partial \mathcal{J}^*}{\partial \mathbf{D}} = 0, & \dfrac{\partial \mathcal{J}^*}{\partial \mathbf{E}} = 0, & \dfrac{\partial \mathcal{J}^*}{\partial \mathbf{Q}^i} = 0, \end{cases} \quad i = 1,2,3,4. \tag{3.8}$$

By solving the system for the unknown vectors $\mathbf{A}$, $\mathbf{B}$, $\mathbf{D}$, $\mathbf{E}$, $\mathbf{Q}^1$, $\mathbf{Q}^2$, $\mathbf{Q}^3$, and $\mathbf{Q}^4$, we obtain an approximate optimal solution for Eq. (1.1). In this study, the "fsolve" tool in Maple 18 is utilized to solve the algebraic system of equations derived in Eq. (3.8). The procedure described above outlines the application of the FCPNN method to the mathematical kidney function model presented in Eq. (1.1).

FCPNN Algorithm for solving a mathematical kidney function model in Eq. (1.1)

Input: Initial conditions, Number of basis functions (m_i, $i = 1,2,3,4$).

* Determine the unknown vectors $\mathbf{A}$, $\mathbf{B}$, $\mathbf{D}$, $\mathbf{E}$ and matrices of CPs coefficients $\mathfrak{U}$, $\mathfrak{V}$, $\mathfrak{P}$ and $\mathfrak{Q}$ based on Eqs. (2.6)-(2.8).
* Determine the basis functions $h_j^i(t)$ by Eq. (2.14).
* Determine the activation functions $\mathbf{S}(t,\mathbf{A})$, $\mathbf{I}(t,\mathbf{B})$, $\mathbf{R}(t,\mathbf{D})$ and $\mathbf{W}(t,\mathbf{E})$ using Eq. (2.15).
* Calculate:
  - The initial conditions Δ_i for $i = 1,2,3,4$ using Eq. (3.2).
  - The residual functions $\mathscr{R}_i$ for $i = 1,2,3,4$ using Eq. (3.3).
  - The 2-norm of the residual functions $\mathfrak{R}\big(\mathbf{A},\mathbf{B},\mathbf{D},\mathbf{E},\mathbf{Q}^1,\mathbf{Q}^2,\mathbf{Q}^3,\mathbf{Q}^4\big)$ using Eq. (3.5).
* Minimize the objective function $\mathfrak{R}\big(\mathbf{A},\mathbf{B},\mathbf{D},\mathbf{E},\mathbf{Q}^1,\mathbf{Q}^2,\mathbf{Q}^3,\mathbf{Q}^4\big)$ under the constraints defined in Eq. (3.6).
* Apply the Lagrange multiplier technique $\mathcal{J}^*[\mathbf{A},\mathbf{B},\mathbf{D},\mathbf{E},\mathbf{Q}^1,\mathbf{Q}^2,\mathbf{Q}^3,\mathbf{Q}^4,\theta]$ using Eq. (3.7).
* Solve the nonlinear algebraic system using Eq. (3.8).

Output: The approximate solutions are: $S(t) \simeq \tilde{S}(t) = S_0 + t\mathbf{S}(t,\mathbf{A})$, $I(t) \simeq \tilde{I}(t) = I_0 + t\mathbf{I}(t,\mathbf{B})$, $R(t) \simeq \tilde{R}(t) = R_0 + t\mathbf{R}(t,\mathbf{D})$, $W(t) \simeq \tilde{W}(t) = W_0 + t\mathbf{W}(t,\mathbf{E})$.

4. Convergence analysis

Theorem 4.1. *Consider the sequence (e_n) be a sequence in a normed linear space $(X,|\cdot|)$ such that $Span\{\mathrm{e}_n|n\in\mathbb{N}\}$ is dense in X. For any element $x_0 \in X$, if (x_n) denotes the best approximation of x_0 within $Span\{\mathrm{e}_1,\ldots,\mathrm{e}_n\}$, then it follows that (x_n) converges to x_0.*

Proof. Since the closure of $Span\{\mathrm{e}_n|n\in\mathbb{N}\}$ is equal to X, there exists a sequence (y_k) in $Span\{\mathrm{e}_n|n\in\mathbb{N}\}$ such that $y_k \to x_0$. Without loss of generality, we can assume that $y_k \in Span\{\mathrm{e}_1,\ldots,\mathrm{e}_{n_k}\}$, for an increasing sequence of natural numbers (n_k). Therefore, we can express the approximations as follows:

$$\|x_{n_k} - x_0\| \le \|y_k - x_0\| \to 0, \ (\text{as } k\to\infty). \tag{4.1}$$

It is also clear that the sequence $(|x_n - x_0|)_{n\in\mathbb{N}}$, composed of non-negative real numbers, is non-increasing. By applying (4.1), this sequence includes a convergent subsequence. Consequently, (x_n) converges to x_0. □

Remark 4.2. *For each $T > 0$, we consider $X = L^2[0,T]$, endowed with the norm $|\cdot|_2$, and let $\mathrm{e}_n := \mathbf{A}_n$ which represents the FCPs. According to Theorem 4.1, it follows that for every $x_0 \in L^2[0,T]$, the sequence(x_n), representing the best approximation of x_0 in $Span\{\mathbf{A}_1,\ldots,\mathbf{A}_n\}$, converges (with respect to $|\cdot|_2$) to x_0.*

5. Existence and uniqueness of solutions for the system (1.1)

Lemma 5.1. *Consider $\Omega \subseteq \mathbb{R}^n$ and define the following differential system*

$$\dot{x}(t) = f(t,x), \quad (t>0), \tag{5.1}$$

with the initial condition x_0. Assume that the function $f : [0,\infty)\times\Omega \to \mathbb{R}^n$ satisfies the locally Lipschitz condition with respect to x on the domain $[0,\infty)\times\Omega$. Under these assumptions, there exists a unique solution $x(t)$ to the differential equation[10, 12].

Theorem 5.2. *For $0<t<\infty$, the system of differential equations (1.1) has a unique solution $\big(S(t),E(t),I(t),R(t)\big)$.*

Proof. Let $F : [0,\infty)\times\mathbb{R}^4 \to \mathbb{R}^4$ be defined for each $t\in[0,\infty)$ and $X=(S,I,R,W)\in\mathbb{R}^3$ by

$$F(t,X) = F(t,S,I,R,W) = \big(f_1(X), f_2(X), f_3(X), f_4(X)\big),$$

where

$$\begin{cases} f_1(X) = a - \beta\left(\frac{W(t)}{W(t)+k}\right)S(t) - \mu S(t), \\ f_2(X) = \beta\left(\frac{W(t)}{W(t)+k}\right)S(t) - (\gamma+\mu)I(t), \\ f_3(X) = \gamma I(t) - \mu R(t), \\ f_4(X) = bW(t)\left(1-\frac{W(t)}{k}\right) - cW(t). \end{cases} \tag{5.2}$$

To prove that (1.1) admits a unique solution, it is sufficient by applying Lemma 5.1 to show that F is locally Lipschitz in the region $[0,T]\times\mathcal{B}$ where M and T are arbitrary positive real numbers and $\mathcal{B} := \{X\in\mathbb{R}^4 : \ \|X\|_\infty \le M\}$. Now, let $X=(S,I,R,W), \tilde{X}=(\tilde{S},\tilde{I},\tilde{R},\tilde{W})\in\mathcal{B}$. Then, it follows that

$$\begin{aligned}
\|F(X)-F(\tilde{X})\|_1 &= \Big|f_1(X)-f_1(\tilde{X})\Big| + \Big|f_2(X)-f_2(\tilde{X})\Big| + \Big|f_3(X)-f_3(\tilde{X})\Big| + \Big|f_4(X)-f_4(\tilde{X})\Big| \\
&= \left|a-\beta\left(\frac{W(t)}{W(t)+k}\right)S(t) - \mu S(t) - \left(a-\beta\left(\frac{\tilde{W}(t)}{\tilde{W}(t)+k}\right)\tilde{S}(t) - \mu\tilde{S}(t)\right)\right| \\
&+ \left|\beta\left(\frac{W(t)}{W(t)+k}\right)S(t) - (\gamma+\mu)I(t) - \left(\beta\left(\frac{\tilde{W}(t)}{\tilde{W}(t)+k}\right)\tilde{S}(t) - (\gamma+\mu)\tilde{I}(t)\right)\right| \\
&+ \left|\gamma I(t) - \mu R(t) - \Big(\gamma\tilde{I}(t) - \mu\tilde{R}(t)\Big)\right| \\
&+ \left|bW(t)\left(1-\frac{W(t)}{k}\right) - cW(t) - \left(b\tilde{W}(t)\left(1-\frac{\tilde{W}(t)}{k}\right) - c\tilde{W}(t)\right)\right| \\
&\le (|\beta|+|\mu|)\Big|S(t)-\tilde{S}(t)\Big| + |\beta|\Big|S(t)-\tilde{S}(t)\Big| + (|\gamma|+|\mu|)\,|\Big|I(t)-\tilde{I}(t)\Big| \\
&+ |\gamma|\Big|I(t)-\tilde{I}(t)\Big| + |\mu|\Big|R(t)-\tilde{R}(t)\Big| + (|b|+|c|)\Big|W(t)-\tilde{W}(t)\Big| \\
&= (2|\beta|+|\mu|)\Big|S(t)-\tilde{S}(t)\Big| + (2|\gamma|+|\mu|)\,|\Big|I(t)-\tilde{I}(t)\Big| \\
&+ |\mu|\Big|R(t)-\tilde{R}(t)\Big| + (|b|+|c|)\Big|W(t)-\tilde{W}(t)\Big| \\
&\le \zeta\Big(\Big|S(t)-\tilde{S}(t)\Big| + \Big|I(t)-\tilde{I}(t)\Big| + \Big|R(t)-\tilde{R}(t)\Big| + \Big|W(t)-\tilde{W}(t)\Big|\Big) \\
&= \zeta\left\|X-\tilde{X}\right\|_1,
\end{aligned}$$

where $\zeta = \max\big\{2|\beta|+|\mu|,\ 2|\gamma|+|\mu|,\ |\mu|,\ |b|+|c|\big\}$. Thus, F is locally Lipschitz. Therefore, by applying Lemma 5.1 the MKFM (1.1) admits a unique solution $\big(S(t),I(t),R(t),W(t)\big)$. □

TABLE 2. The runtime (in seconds) of the FCPNN method with several values of m_i, $i = 1, 2, 3, 4$.

case	m_1	m_2	m_3	m_4	CPU times (case a)	CPU times (case b)	CPU times (case c)
1	2	2	2	2	4.34	4.32	4.34
2	3	3	3	3	7.41	7.42	7.43
3	3	3	4	4	11.18	11.19	11.19

TABLE 3. The optimal residual function values for various m_i settings, where $i = 1, 2, 3, 4$.

case	m_1	m_2	m_3	m_4	Residual function (case a)	Residual function (case b)	Residual function (case c)
1	2	2	2	2	$1.7235E-07$	$3.6628E-07$	2.2976E-07
2	3	3	3	3	$6.5932E-08$	$2.1385E-08$	4.2893E-08
3	3	3	4	4	$1.4062E-10$	$9.9562E-11$	6.5674E-11

6. SOLUTION METHOD AND APPROXIMATE RESULTS

In this section, we validate and demonstrate the applicability of the proposed strategy for solving MKFM in Eq. (1.1). All numerical calculations are performed using Maple 2024, and the CPU time (in seconds) is reported for an Intel Core i7 3.00GHz personal computer with 8 GB of RAM. Since the analytical solution for the given problem is unknown, we verify the reliability and accuracy of the technique by analyzing the residual error function. To create the figures of the approximations obtained for $S(t)$, $I(t)$, $R(t)$ and $W(t)$, we consider the following initial and parameter values:

$$\begin{aligned}
&Case\ a: S_0 = 0.1,\ I_0 = 0.2,\ R_0 = 0.3,\ W_0 = 0.4,\ \mu = \frac{1}{65},\ \gamma = \frac{1}{45},\ \beta = \frac{1}{100},\ k = 60,\ a = 2,\ b = \frac{1}{10},\ c = \frac{2}{5},\\
&Case\ b: S_0 = 0.1,\ I_0 = 0.2,\ R_0 = 0.3,\ W_0 = 0.4,\ \mu = \frac{1}{65},\ \gamma = \frac{1}{45},\ \beta = \frac{1}{100},\ k = 60,\ a = 2,\ b = \frac{1}{4},\ c = \frac{1}{10},\\
&Case\ c: S_0 = 0.1,\ I_0 = 0.2,\ R_0 = 0.3,\ W_0 = 0.4,\ \mu = \frac{1}{28},\ \gamma = \frac{1}{34},\ \beta = \frac{1}{70},\ k = 63,\ a = 2.1,\ b = \frac{1}{2},\ c = \frac{1}{15}.
\end{aligned} \tag{6.1}$$

The results obtained are illustrated in Figs. 1-4 with $m_1 = m_2 = 3$ and $m_3 = m_4 = 4$ for case a (left-up), case b (right-up) and case c (right-down) over a time period of one month. The runtime (in seconds) for the our suggested technique and the optimal values for our proposed technique, along with the optimal values for the residual function for various m_1, m_2, m_3 and m_4 values are presented in Tables 2 and 3.

Figure 1 illustrates the increase in the susceptible human population over time with the growing human population in cases a, b and c. Figure 2 demonstrates that the ratios of magnesium and calcium in water, and consequently the infected human population, decrease over time due to water treatment procedures in cases a, b and c. Figure 3 indicates that the recovered concentrations of calcium and magnesium in water decrease over time in cases a, b and c. Figure 4 reveals that the recovered concentrations of calcium and magnesium decrease over time in case a, while in cases b and c, they increase due to higher concentrations of these minerals in the water and fewer treatment procedures.

The approximate solutions of $S(t)$, $I(t)$, $R(t)$ and $W(t)$ obtained using our method with $m_1 = m_2 = m_3 = m_4 = 2$ for cases a, b, and c are as follows:
Case a:

$$\begin{cases}
\tilde{S}(t) = 0.1 - t.arcsinh(-3.61629 - 0.29144t^{1.71208} + 0.34399t^{1.60921}),\\
\tilde{I}(t) = 0.2 - t.arcsinh(0.00701 + 0.00153t^{1.75336} - 0.00122t^{2.87777}),\\
\tilde{R}(t) = 0.3 - t.arcsinh(-0.00009 + 0.00082t^{1.40353} - 0.00049t^{2.77711}),\\
\tilde{W}(t) = 0.4 + t.arcsinh(-0.12095 + 0.01729t^{0.91297} - 0.00037t^{2.42200}).
\end{cases} \tag{6.2}$$

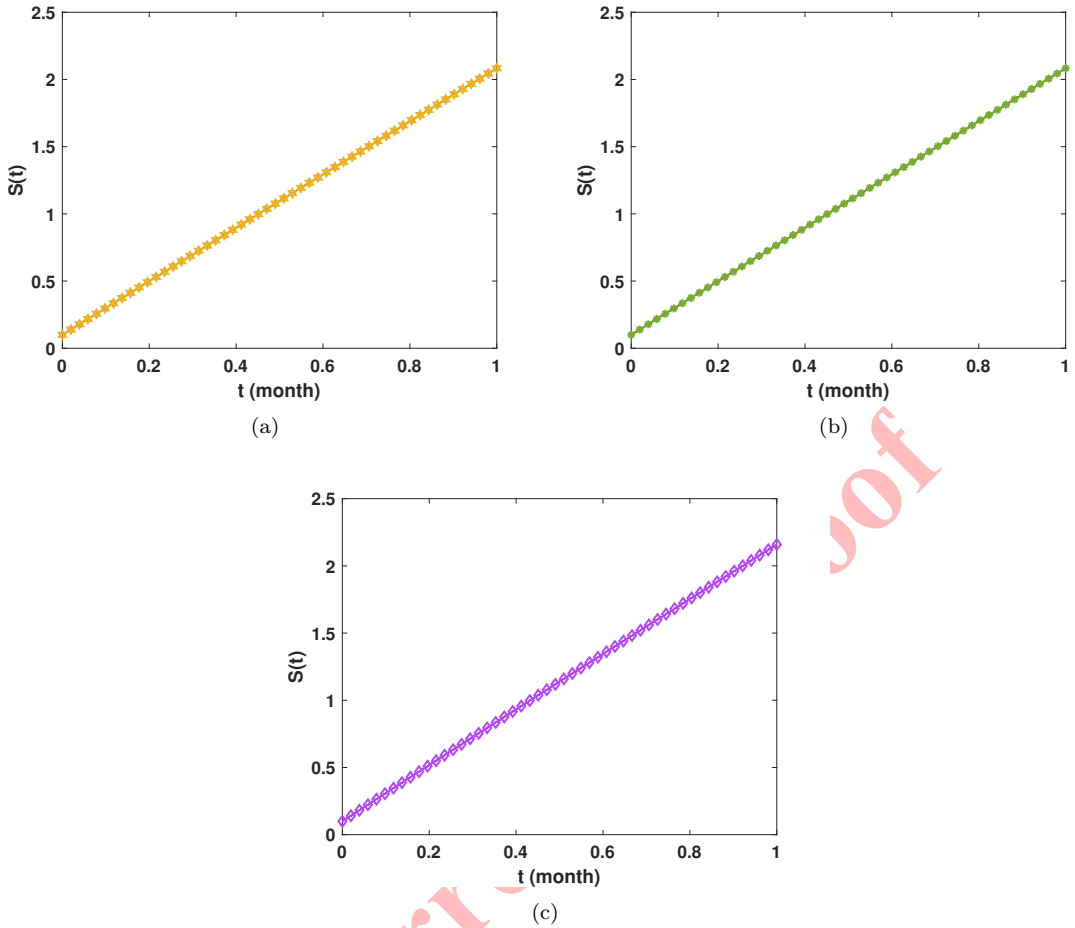

FIGURE 1. FCPNN solutions of $S(t)$ with $m_1 = m_2 = 3$ and $m_3 = m_4 = 4$ for case a (top left), case b (top right), and case c (bottom right) over a time period of one month.

Case b:

$$\begin{cases} \tilde{S}(t) = 0.1 - t.arcsinh(-3.61196 - 0.29497t^{2.16243} + 0.34321t^{2.01089}), \\ \tilde{I}(t) = 0.2 + t.arcsinh(-0.00747 + 0.00028t^{1.79706} - 0.00011t^{2.85747}), \\ \tilde{R}(t) = 0.3 - t.arcsinh(0.00018 + 0.00011t^{1.81142} - 0.00004t^{2.86150}), \\ \tilde{W}(t) = 0.4 + t.arcsinh(0.06012 + 0.00615t^{1.80852} - 0.00232t^{2.88333}). \end{cases} \tag{6.3}$$

Case c:

$$\begin{cases} \tilde{S}(t) = 0.1 - t.arcsinh(-3.99810 - 0.15128t^{1.69211} + 0.29298t^{1.36213}), \\ \tilde{I}(t) = 0.2 + t.arcsinh(-0.01293 + 0.00063t^{1.63624} - 0.00018t^{2.76380}), \\ \tilde{R}(t) = 0.3 - t.arcsinh(0.00487 + 0.00007t^{1.69478} - 0.000007t^{2.80692}), \\ \tilde{W}(t) = 0.4 + t.arcsinh(0.17329 + 0.03975t^{1.04680} + 0.00312t^{2.66238}). \end{cases} \tag{6.4}$$

The mathematical kidney function model (1.1) is also solved using the techniques discussed in section 4, but with the CPNN approach. Table 4 lists the values obtained for the optimal residual function in relation to m_1, m_2, m_3 and

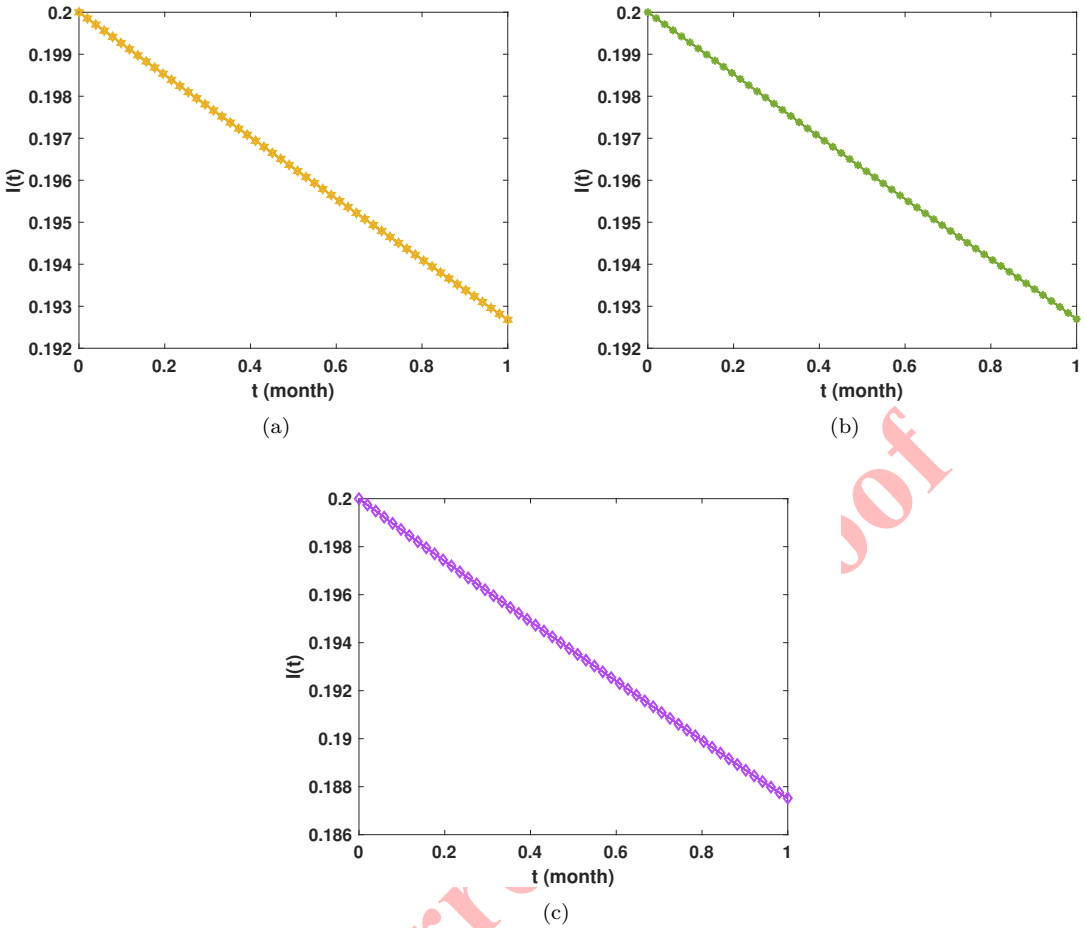

FIGURE 2. FCPNN solutions of $I(t)$ with $m_1 = m_2 = 3$ and $m_3 = m_4 = 4$ for case a (top left), case b (top right), and case c (bottom right) over a time period of one month.

TABLE 4. The optimal residual function values for case c and various m_i settings using CPNN and FCPNN, where $i = 1, 2, 3, 4$.

case	m_1	m_2	m_3	m_4	Residual function (CPNN)	Residual function (FCPNN)
1	2	2	2	2	$3.5258E-03$	$2.2976E-07$
2	3	3	3	3	$7.6253E-04$	$4.2893E-08$
3	3	3	4	4	$1.8552E-06$	$6.5674E-11$

m_4 using both CPNN and FCPNN for case c. The results presented in Table 4 indicate that the proposed method is more accurate than those based on CPNN.

7. CONCLUDING REMARKS

In conclusion, the discussion highlights the effectiveness of combining the neural network approach with clique polynomials (FCPs) to solve MKFM. We introduced a novel modification of clique polynomials to achieve optimal

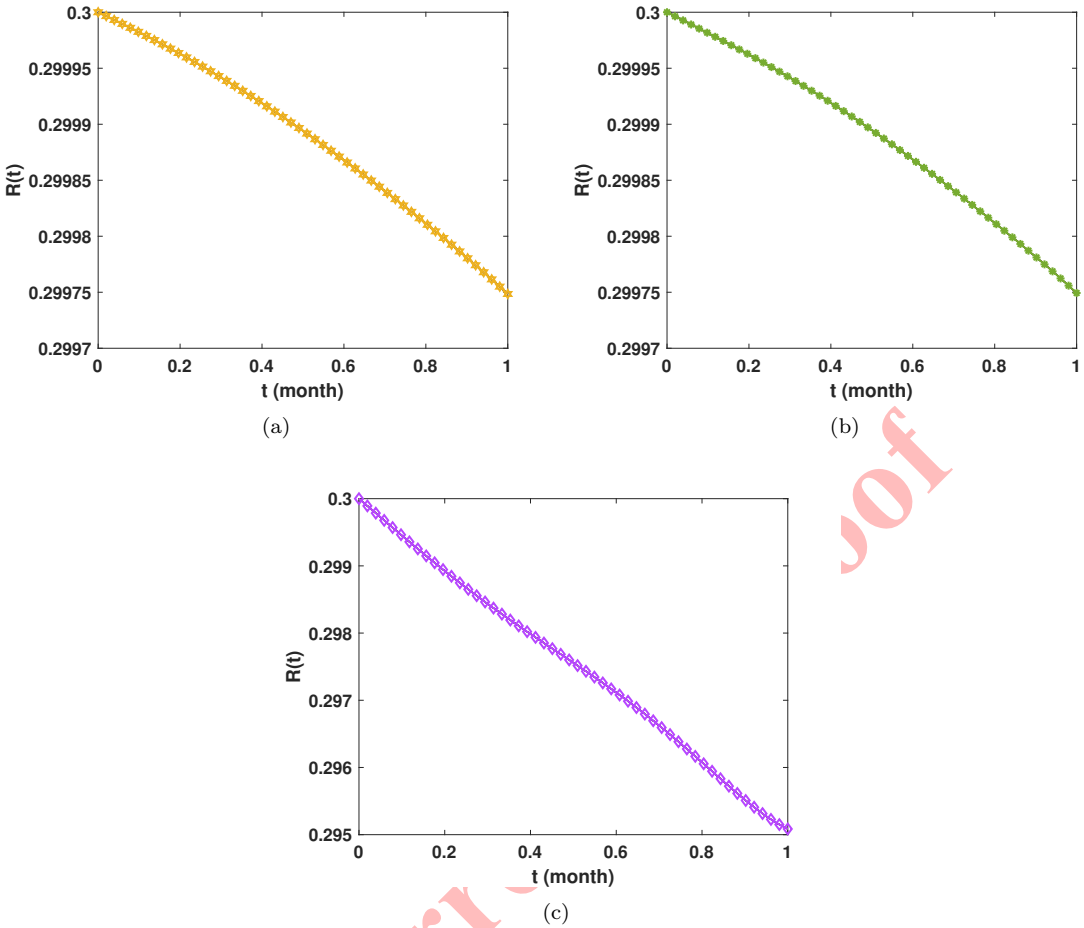

FIGURE 3. FCPNN solutions of $R(t)$ with $m_1 = m_2 = 3$ and $m_3 = m_4 = 4$ for case a (top left), case b (top right), and case c (bottom right) over a time period of one month.

solutions for MKFM. Our central hypothesis posited that this method leverages function approximation to yield more precise and efficient solutions in the form of FCPs. By employing a suitable neural network approach, we approximated unknown coefficients and parameters for the solution function. The validity of our method rests on the assumption that the convergence rate improves significantly with an increased number of basis functions. Additionally, numerical experiments are presented to enhance understanding of the method and to demonstrate the step-by-step process for solving MKFM, making the concepts more tangible and accessible. This foundational work paves the way for future research to expand the framework using optimization methods and various bioscience models, potentially enhancing the accuracy and flexibility of neural network models across different domains.

DECLARATIONS

Data availability Statement: All data produced or analyzed in this study are contained within the submitted article.
Funding: No financial support, grants, or other funding was received for this work.
Ethics approval and consent to participate: Not applicable.
Author contributions: Each author made an equal contribution to all aspects of this study.

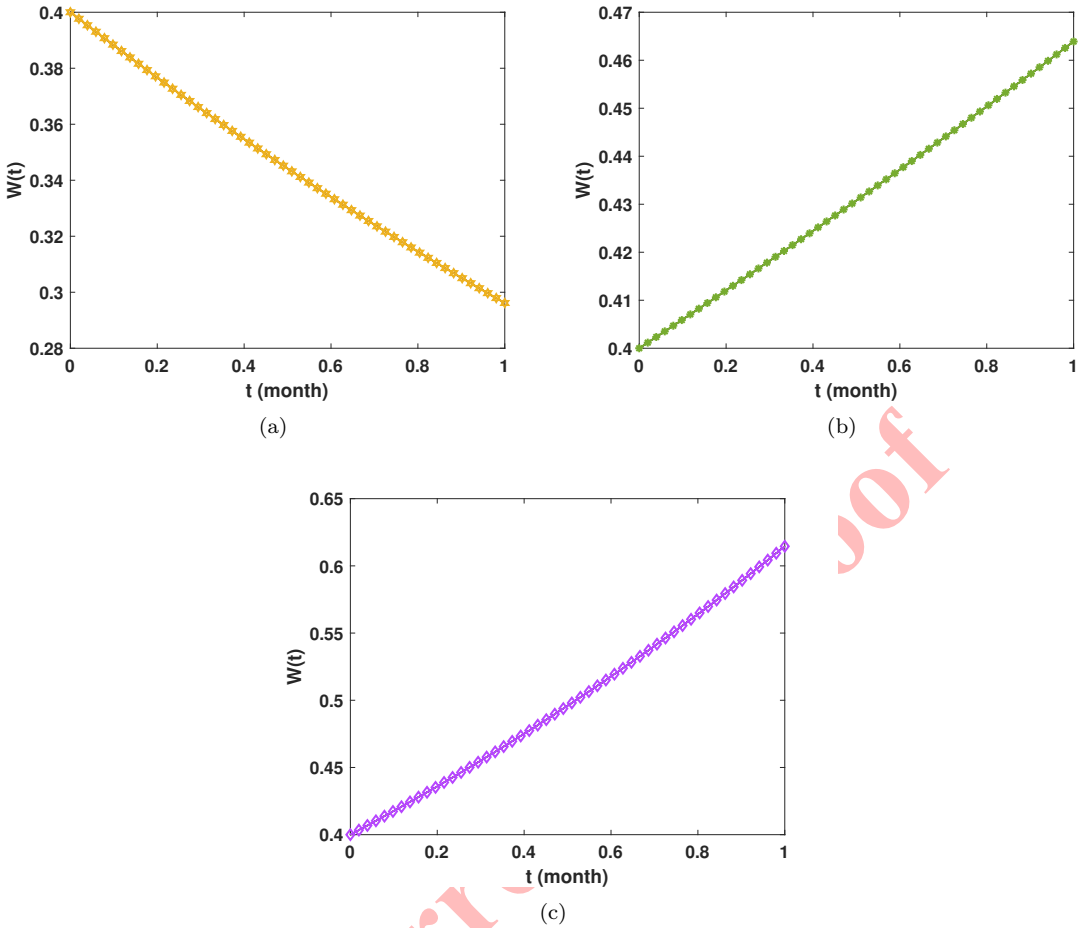

FIGURE 4. FCPNN solutions of $W(t)$ with $m_1 = m_2 = 3$ and $m_3 = m_4 = 4$ for case a (top left), case b (top right), and case c (bottom right) over a time period of one month.

Consent to publish: All co-authors have given consent for the submission.
Competing Interests: Authors declare no competing interests.

REFERENCES

[1] F. Asadi-Mehregan, P. Assari, and M. Dehghan, *Numerical simulation of spatio-temporal spread of an infectious disease utilizing a collocation method based on local radial basis functions*, Engineering with Computers, *40* (2024), 2473–2496.
[2] Y. Bao, Y. Li, Y. Zhou, et al., *Water quality and neurodegenerative disease risk in the middle-aged and elderly population*, Ecotoxicology and Environmental Safety, *289* (2025), 117647.
[3] Z. Chen, Z. Yang, and D. Sheng, *Numerical analysis of linearly implicit Euler method for age-structured SIS model*, Journal of Applied Mathematics and Computing, *70* (2024), 969–996.
[4] J. He, *A new high-precision numerical method for solving the HIV infection model of CD4(+) cells*, Physica A: Statistical Mechanics and its Applications, *653* (2024), 130090.
[5] B. He, W. Hu, K. Zhang, et al., *Image segmentation algorithm of lung cancer based on neural network model*, Expert Systems, *39*(3) (2022), e12822.

[6] F. Hossienifar, M. Entezari, and S. Hosseini, *Water hardness zoning of Isfahan Province, Iran, and its relationship with cardiovascular mortality*, ARYA Atherosclerosis, *15*(6) (2019), 275–280.
[7] R. Jasevicius, *Numerical modeling of red blood cell interaction mechanics*, Mechanics of Advanced Materials and Structures, *30*(12) (2022), 2524–2531.
[8] N. Jeeva and K. M. Dharmalingam, *Numerical analysis and artificial neural networks for solving nonlinear tuberculosis model in SEITR framework*, Advanced Theory and Simulations, *8* (2025), 2401287.
[9] M. Li and Z. Yang, *Numerical analysis of an age-structured model for HIV viral dynamics with latently infected T cells based on collocation methods*, Mathematics and Computers in Simulation, *230* (2025), 289–305.
[10] Y. Li, Y. Chen, and I. Podlubny, *Stability of fractional-order nonlinear dynamic systems: Lyapunov direct method and generalized Mittag-Leffler stability*, Computers and Mathematics with Applications, *59* (2010), 1810–1821.
[11] G. Li, B. Chen, and X. Wang, *Numerical investigation on red blood cell flow based on unstructured grid*, International Journal for Numerical Methods in Biomedical Engineering, *39*(11) (2023), e3647.
[12] C. Maji, D. Mukherjee, and D. Kesh, *Study of a fractional-order model of chronic wasting disease*, Mathematical Methods in the Applied Sciences, *43*(7) (2020), 4669–4682.
[13] F. Movahedi, *Stability analysis and numerical approximate solution for a new epidemic model with the vaccination strategy*, Mathematical Methods in the Applied Sciences, *47*(7) (2024), 6403–6414.
[14] A. Pandey and S. Ghosh, *Numerical study of childhood disease model with Lyapunov stability analysis*, Indian Journal of Physics, *99* (2025), 1–12.
[15] B. Prakash, A. Setia, S. Bose, and R. P. Agarwal, *Error analysis of a Haar wavelets-based numerical method with its application to a nonlinear fractional dengue model*, International Journal of Computer Mathematics, *101*(12) (2022), 1379–1397.
[16] P. Rahimkhani, Y. Ordokhani, and M. Razzaghi, *Fractional-order clique functions to solve left-sided Bessel fractional integro-differential equations*, Chaos, Solitons and Fractals, *192* (2025), 116025.
[17] P. Sengupta, *Potential health impacts of hard water*, International Journal of Preventive Medicine, *4*(8) (2013), 866–875.
[18] M. Z. Ullah, A. K. Alzahrani, and D. Baleanu, *An efficient numerical technique for a new fractional tuberculosis model with nonsingular derivative operator*, Journal of Taibah University for Science, *13*(1) (2019), 1147–1157.
[19] Z. Wang, Z. Yang, G. Yang, and C. Zhang, *Numerical analysis of age-structured HIV model with general transmission mechanism*, Communications in Nonlinear Science and Numerical Simulation, *134* (2024), 108020.
[20] J. Zhang, H. Luo, H. Wu, et al., *The association between domestic water hardness and kidney stone disease: a prospective cohort study from the UK Biobank*, International Journal of Surgery, *111*(2) (2025), 1957–1967.
[21] M. Yousefi, H. Najafi Saleh, M. Yaseri, et al., *Association of consumption of excess hard water, body mass index and waist circumference with risk of hypertension in individuals living in hard and soft water areas*, Environmental Geochemistry and Health, *41*(3) (2019), 1213–1221.